



# Morphology and photocatalytic performance of nano-sized TiO<sub>2</sub> prepared by simple hydrothermal method with different pH values

Hao Xu, Shi-Qi Liu, Shan Zhou, Tang-Zhi-Jiu Yuan, Xiang Wang,  
Xia Tang, Jian Yin, Hui-Jin Tao\* 

Received: 5 September 2016 / Revised: 22 December 2016 / Accepted: 5 September 2017 / Published online: 4 October 2017  
© The Nonferrous Metals Society of China and Springer-Verlag GmbH Germany 2017

**Abstract** pH value is a key factor in the preparation of nano-sized TiO<sub>2</sub> with hydrothermal method. Using Ti(SO<sub>4</sub>)<sub>2</sub> as the titanium source, H<sub>2</sub>O<sub>2</sub> as the complexing agent, NaOH and HCl as the pH value regulator, nano-sized TiO<sub>2</sub> powder with various morphologies and sizes was synthesized. Changes in morphology, size and phase type with pH values of samples were characterized by X-ray diffraction (XRD) and transmission electron microscopy (TEM) measurements. Results show that under the present preparation conditions, TiO<sub>2</sub> powder is an anatase phase with pH value less than 11, but is more likely to be a brookite phase with pH value more than 11. With the increase in pH value from 1 to 11 in hydrothermal environment, nano-sized anatase TiO<sub>2</sub> gradually grows up in all directions. {001}, {101} and {100} groups of crystal plane are the exposed crystal planes of nano-sized anatase TiO<sub>2</sub> for the (004), (101) and (200) facets found in high-resolution TEM image. The photocatalytic performance of nano-sized TiO<sub>2</sub> with different morphologies was compared by measuring their photocatalytic degradation rates for methylene blue under ultraviolet light. Results show that anatase TiO<sub>2</sub> prepared under the alkaline

hydrothermal environment (pH = 9, 11) has a better photocatalytic degrading performance. Different sizes and phases of nanoscaled TiO<sub>2</sub> powders with different photocatalytic performances can be prepared by the control of pH value of hydrothermal solutions.

**Keywords** Hydrothermal method; pH value; Anatase; Brookite; Nano-sized crystal morphology

## 1 Introduction

Titanium dioxide (TiO<sub>2</sub>) is the most popular semiconductor material in the field of purification of polluted water and air for its high stability, good optical property, photoelectric effect and low toxicity [1, 2]. The optical properties and photoelectric effect of TiO<sub>2</sub> depend on the morphology of crystals, active surface ratio, crystalline size, phase composition and distribution [3]. How to control the morphology and structure of TiO<sub>2</sub> to make an improvement on the photocatalytic performance is a hot spot of such research field.

Currently, thermal vapor condensation and liquid-phase preparation are the two main methods in the preparation of TiO<sub>2</sub> powders. The sol-gel and hydrothermal preparation methods are the most frequently used methods in liquid-phase preparation [4]. In such methods, the nano-powder can be prepared after heat treatment of precipitation with proper precipitant or by crystallization of compounds in solutions with hydrolysis method [5]. Because of the simplicity of process and the controllability of morphology, composition and structure, these methods are always used for the preparation of TiO<sub>2</sub> nano-powders, but the influence

---

H. Xu, S.-Q. Liu, S. Zhou, T.-Z.-J. Yuan, X. Wang, X. Tang,  
H.-J. Tao\*

School of Material Science and Engineering, Central South University, Changsha 410083, China  
e-mail: thj@csu.edu.cn

J. Yin

State Key Laboratory for Powder Metallurgy, Central South University, Changsha 410083, China

H.-J. Tao

Key Lab of Nonferrous Materials Science and Engineering, Ministry of Education, Central South University, Changsha 410083, China

of many factors such as temperature, pH value and time on the microstructure and morphology of is still unclear.

The pH value of precursor solution has a vital effect on the morphology and phase of TiO<sub>2</sub> for both the sol–gel and hydrothermal preparation methods [6]. Zhou et al. [7] prepared nano-sized TiO<sub>2</sub> by sol–gel method and found that pH value of different precursor solutions can apparently affect crystal growth habits, phase compositions and grain sizes. Li [8] prepared TiO<sub>2</sub> by the sol–gel method as well and found that the anatase-phase TiO<sub>2</sub> can be prepared in the weakly acidic condition, but the rutile phase can be formed in the strong acidic condition. Devi et al. [9] found that the phase type of TiO<sub>2</sub> would transfer from anatase to rutile when the pH value increases in the sol–gel method. Gao and Chen [10] found that pH value can affect the phase type of TiO<sub>2</sub> doped with other elements. Similarly, pH value is a key factor to produce nano-size with different sizes and morphologies as nano-belts or nano-rods in the preparation process by hydrothermal method [11–13].

Zhou et al. [14] found that the rutile phase of TiO<sub>2</sub> can be formed easily in the acidic condition, while the anatase phase is more accessible in the neutral and weakly acidic condition [15]. Zhu et al. [16] discovered that titanate fiber transformed to anatase and rutile phases in the acidic solutions during the hydrothermal process related to two kinds of possible mechanisms. Yao et al. [17] prepared brookite phase of TiO<sub>2</sub> by regulating the pH value of hydrothermal solution. Testino et al. [18] found that pH value plays an important role in the morphology, size and phase type of nano-sized TiO<sub>2</sub> in hydrothermal synthesis process.

In this work, nano-sized TiO<sub>2</sub> was prepared by hydrothermal method. The morphologies, sizes and phase types of samples with pH value changing from 1 to 13 were compared, and the influence mechanism of pH value on such properties was studied. Finally, the different photocatalytic effects of these samples on the degradation of methylene blue (MB) under ultraviolet light were explored furthermore.

## 2 Experimental

### 2.1 Materials and equipments

Ti(SO<sub>4</sub>)<sub>2</sub> (CP, ≥96.0 wt%) used as the Ti source was bought from Sinopharm Chemical Reagent Co., Ltd. Hydrogen peroxide (H<sub>2</sub>O<sub>2</sub>, AR, ≥30.0 wt%) was bought from West Long Chemical Co., Ltd. NH<sub>3</sub>·H<sub>2</sub>O (AR, ≥99.0 wt%) was bought from Zhuzhou Research Institute of Chemical Industry. Hydrochloric acid (HCl, AR, 36 wt%–38 wt%) was bought from Zhuzhou Research Institute of Chemical Industry. Absolute ethyl (C<sub>2</sub>H<sub>5</sub>OH,

AR, ≥99.7 wt%) was bought from Hunan Hui Hong Reagent Co., Ltd. Polyethylene glycol 200 (PEG200, AR) used as the modification agent was bought from Tianjin Guangfu Fine Chemical Research Institute. Sodium hydroxide (NaOH, AR, ≥96 wt%) was bought from Tianjin Fengchuan Reagent Technologies Co., Ltd. PHS-3C type pH meter used in this experiment was bought from Shanghai Yidian Science Instrument.

### 2.2 Hydrothermal synthesis of nano-sized titanium dioxide

2 g Ti(SO<sub>4</sub>)<sub>2</sub> powder was dissolved into 70 ml distilled water. The solution was placed in a magnetic agitator at 70 °C and stirred for 10 min, then the dilute ammonia water was added (25 wt%) into it till pH = 7.5. Moderate distilled water was added into the solution and then it was placed in a centrifugal machine (10,000 r·min<sup>-1</sup>) three times with 10 min each time. The centrifuged precipitate was placed in a beaker, and 40 ml distilled water was added. The mixture in the beaker was put in a magnetic agitator under room temperature and stirred by dripping hydrogen peroxide (30.0 wt%) until the pH value reached 7 and the color of solution became yellow. 40 ml PEG200 was added into the solution for uniform mixing and then the solution was cooled down to room temperature. Hydrochloric acid and sodium hydroxide with certain concentrations were used to adjust the pH value (1, 3, 5, 7, 9, 11, 13). These pH values of reaction solution were tested by pH meter. The hydrothermal solution was put in an ultrasonic cleaning machine and dispersed ultrasonically for 10 min. Then, the hydrothermal solution was transferred into hydrothermal synthesis reactors (60%–80% filled) for 7 h under the temperature of 180 °C. After centrifugal cleaning, hydrothermal products were dried at 60 °C to attain powder samples. Samples were ground and then put in bags for characterizations.

### 2.3 Characterization of nano-sized titanium dioxide

The crystalline structure of titanium dioxide was characterized by X-ray diffraction meter (XRD, Rigaku D/Max 2500) using Cu K $\alpha$  radiation ( $\lambda = 0.15418$  nm). The scanning angle range was 10°–80°, and scanning speed was 8(°)·min<sup>-1</sup>. The morphology of titanium dioxide was characterized by transmission electron microscope (TEM, JEOL JEM-2100F). Before observation of TEM, a certain amount of sample was dissolved in anhydrous ethanol and dispersed by the ultrasonic wave. One or two drops of such liquid were added on the ultrathin carbon film for drying and the subsequent characterization.

## 2.4 Photoactivity evaluation

Photocatalytic device was the catalytic cold trap. Procedure of photocatalytic experiments was as follows: 400 ml MB solution with the concentration of  $10 \text{ mg}\cdot\text{L}^{-1}$  was measured and mixed with 0.1 g  $\text{TiO}_2$  powder. The solution and photocatalyst were mixed completely and thoroughly by a magnetic stirrer. After stirring for 10 min for the establishment of adsorption equilibrium, 8–10 ml liquid was measured into a test tube and placed in the dark. The mercury lamp ( $\lambda = 365 \text{ nm}$ ) was then turned on at the beginning of photocatalytic degradation. The mercury lamp was stopped every 5 min to measure 8–10 ml liquid, and 40 min was set as the final. The photoactivity was evaluated at the degradation rate of MB by different nano-sized  $\text{TiO}_2$ . The luminousness of the MB solution at  $\lambda = 664 \text{ nm}$ , which is the characteristic absorption peak of MB, was measured by a 752 N ultraviolet–visible (UV–Vis) spectrophotometer according to the Lambert–Beer formula, and the concentrations of MB at different time during photocatalytic reaction can be calculated via this formula:

$$A = -\lg T = -\lg \frac{I}{I_0} = k \cdot c \quad (1)$$

where  $A$  is the light absorbance of solution,  $T$  is the transmittance,  $I_0$  and  $I$  are, respectively, the initial and final light intensity when light passes the solution,  $k$  is a constant and  $c$  is the concentration of solution. Degradation rate ( $D$ ) of MB is shown as:

$$D = \frac{c_t - c_0}{c_0} \times 100\% \quad (2)$$

where  $c_0$  and  $c_t$  are, respectively, the concentration of MB before and after photocatalysis for time  $t$ . The degradation rate–time diagram can then be drawn according to a series of  $D$  values.

## 3 Results and discussion

### 3.1 Hydrothermal synthesis of nano-sized $\text{TiO}_2$

$\text{TiO}_2$  nano-powder samples labeled from 1 to 10 in different pH values were prepared according to the experimental process in Sect. 2.2, and samples labeled from 11 to 15 are the comparison group with the change in modification agent, hydrothermal temperature or hydrothermal time. Samples 11 and 15 were compared with Sample 4 in modification agent and temperature, respectively. Samples 12, 13 and 14 were compared with Sample 7 in modification agent, hydrothermal time and temperature,

respectively. All the samples and their hydrothermal conditions are shown in Table 1.

### 3.2 Structure and phase of nano-sized $\text{TiO}_2$

Figure 1a is the XRD patterns of Samples 1–6, which shows that all these samples are characterized as the anatase phase without other phase. If  $H$  is the average thickness of the grain parallel to the normal direction of crystal plane, it can be calculated by Debye–Scherrer formula:

$$H = \frac{K\gamma}{B \cos \theta} \quad (3)$$

where  $K$  is Scherrer Constant,  $\gamma$  is the wave length of X-ray,  $B$  stands for the FWHM of diffraction peak and  $\theta$  is the diffraction angle. According this formula, the thickness along the corresponding direction of crystal planes will increase with the decrease in FWHM, indicating that the crystal sizes of anatase  $\text{TiO}_2$  will increase with the increase in pH values since the values of FWHM decrease and the intensities of (101), (004), (200) planes increase with the increase in pH value in Fig. 1a.

Figure 1b is XRD patterns of Samples 6–10. The characteristic peak of (211) plane of brookite  $\text{TiO}_2$  does not appear until pH value increases to 11.5. And from pH = 11.5 to pH = 13.0, the samples are all characterized as the brookite phase. But for the case of pH = 11.0, it is anatase, so there may exist a critical pH value between 11.0 and 11.5 for the phase transformation between anatase and brookite under present preparation conditions.

**Table 1** Samples and hydrothermal conditions

Samples	pH	Modification agent	Temperature/ $^{\circ}\text{C}$	Time/h
1	1	PEG200	180	7
2	3	PEG200	180	7
3	5	PEG200	180	7
4	7	PEG200	180	7
5	9	PEG200	180	7
6	11	PEG200	180	7
7	13	PEG200	180	7
8	11.5	PEG200	180	7
9	12	PEG200	180	7
10	12.5	PEG200	180	7
11	7	Distilled water	180	7
12	13	Distilled water	180	7
13	13	PEG200	180	24
14	13	PEG200	260	7
15	7	PEG200	260	7

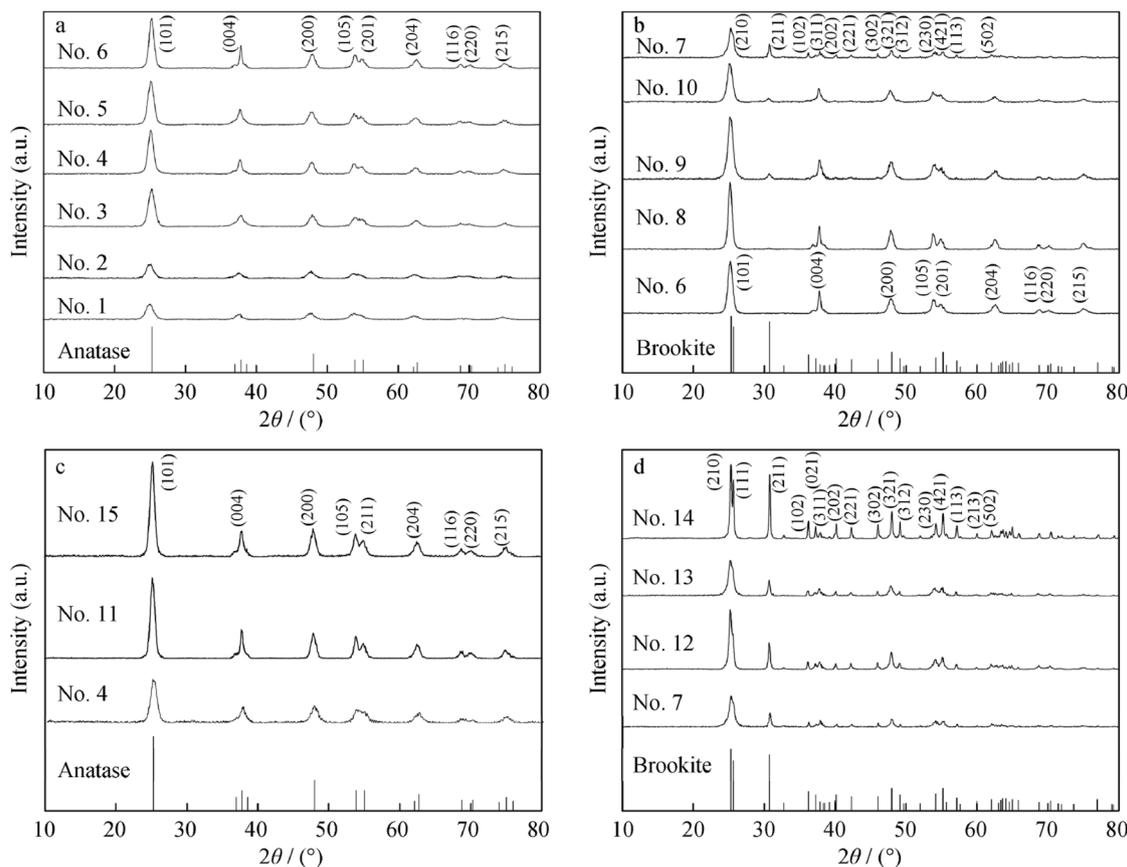


**Fig. 1** XRD Patterns of **a** Samples 1–6, **b** Samples 6–10, **c** Samples 4, 11 and 15 and **d** Samples 7, 12, 13 and 14

Figure 1c is XRD patterns of Samples 4, 11 and 15. All of them are characterized as anatase phase. Compared with Sample 4, Sample 11 was prepared without any modification agent, indicating that the places of non-uniform nucleation decrease and then the nucleation rate and grain size decrease [19]. Sample 15 was prepared at a higher temperature than other samples, so its diffraction peak of each plane is higher and its FWHM is thinner than those of other samples with the grain size larger in terms of Eq. (3).

Figure 1d is XRD patterns of Samples 7, 12, 13 and 14. All of them were prepared in the condition of pH = 13.0. It is found that the grain size increases when there are no modification agents, temperature increases or time prolongs.

In summary, hydrothermal temperature, time and modification agent have an obvious effect on the grain morphology and size of TiO<sub>2</sub>, but they have no effect on the phase type of TiO<sub>2</sub> under present experimental conditions. It is the pH value that has effect on the phase transformation from anatase to brookite for nano-TiO<sub>2</sub> [20].

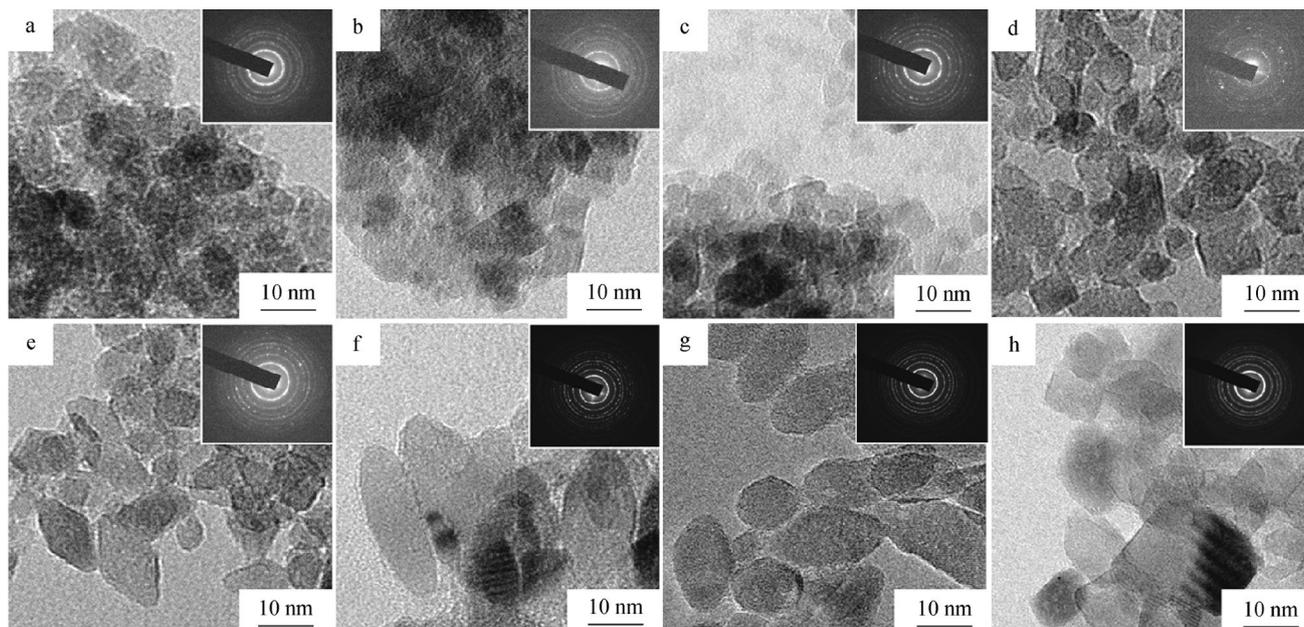
### 3.3 Morphologies of nano-TiO<sub>2</sub>

#### 3.3.1 Morphologies and sizes of nano-TiO<sub>2</sub> grains

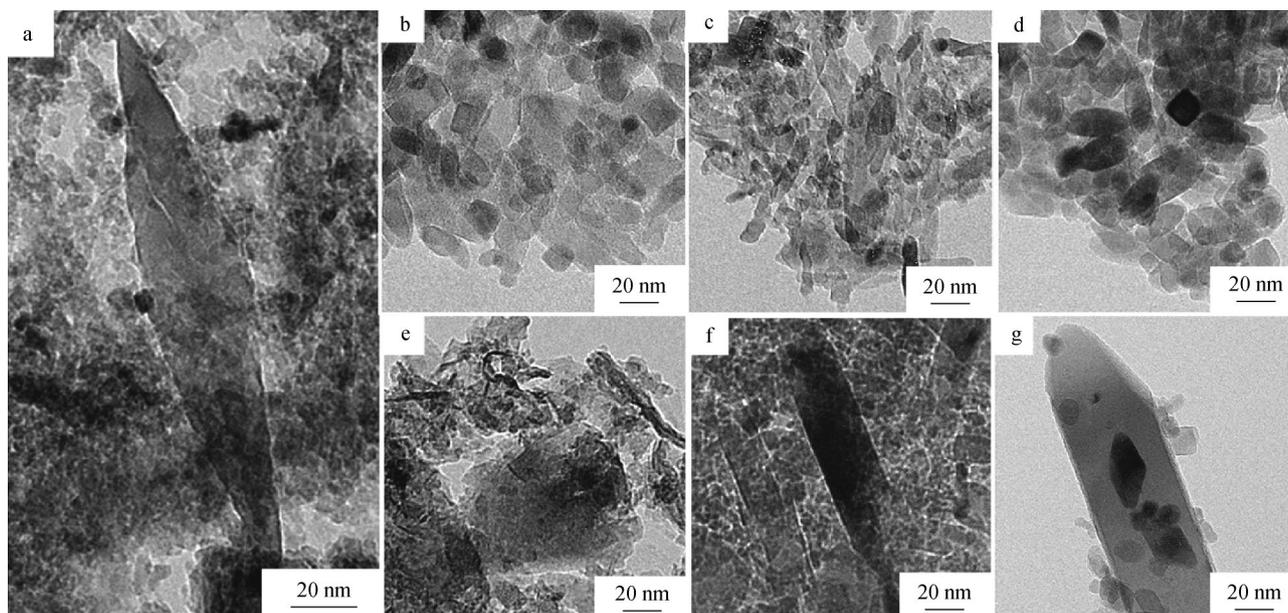
In the discussion of Sect. 3.2, Samples 1–6, 11 and 15 are all anatase TiO<sub>2</sub>, and Samples 7–12 and 14 are brookite TiO<sub>2</sub>. TEM images in Figs. 2 and 3 agree well with these results from XRD analyses. In Fig. 2, all these TEM images are shown as anatase phase.

Figure 2a–f (Samples 1–6) shows that the sizes of TiO<sub>2</sub> particles prepared in the acidic condition are less than 10 nm, and with the increase in pH value, grains grow in every direction and the sizes increase constantly. In TEM image, compared with that of Sample 4 (Fig. 2d), the grain sizes of Sample 11 (Fig. 2g) and Sample 15 (Fig. 2h) are larger, proving that the influence of modification agent and hydrothermal temperature on the size of the crystals is consistent with that from XRD results. The diffraction disks on the top right corner of each image manifest that the crystallinity of every grain is good.

Figure 3 is the TEM images of brookite TiO<sub>2</sub>. The morphologies of Samples 7–10 are all long or lath strips which are the typical morphology of brookite, and the



**Fig. 2** TEM images and diffraction patterns of anatase  $\text{TiO}_2$ : **a** Sample 1, **b** Sample 2, **c** Sample 3, **d** Sample 4, **e** Sample 5, **f** Sample 6, **g** Sample 11 and **h** Sample 15



**Fig. 3** TEM images of brookite  $\text{TiO}_2$ : **a** Sample 7, **b** Sample 8, **c** Sample 9, **d** Sample 10, **e** Sample 12, **f** Sample 13 and **g** Sample 14

phase is brookite as proved by XRD results. When  $\text{TiO}_2$  is shown as brookite, the length of  $\text{TiO}_2$  grains will be longer with the increase in pH value. It is found from Fig. 2a–f (pH = 1, 3, 5, 7, 9, 11) and Fig. 3a (pH = 13) that under the same hydrothermal condition, the morphologies, sizes and phases of nano- $\text{TiO}_2$  vary with the pH values.

In summary, when pH = 1–11, the sizes of nano- $\text{TiO}_2$  grains will increase with the increase in pH value. Combining with XRD results, there may be a critical point in pH

range of 11.0–11.5 for phase transformation. When pH value is larger than this point, the product is brookite  $\text{TiO}_2$  and the size of brookite grain will change apparently with pH value.

### 3.3.2 Crystalline shape of nano-sized $\text{TiO}_2$

Figure 3 shows TEM images of anatase  $\text{TiO}_2$  of Samples 1–6, 11 and 15. (004), (200) and (101) planes can be calibrated after corresponding crystal plane calibration in

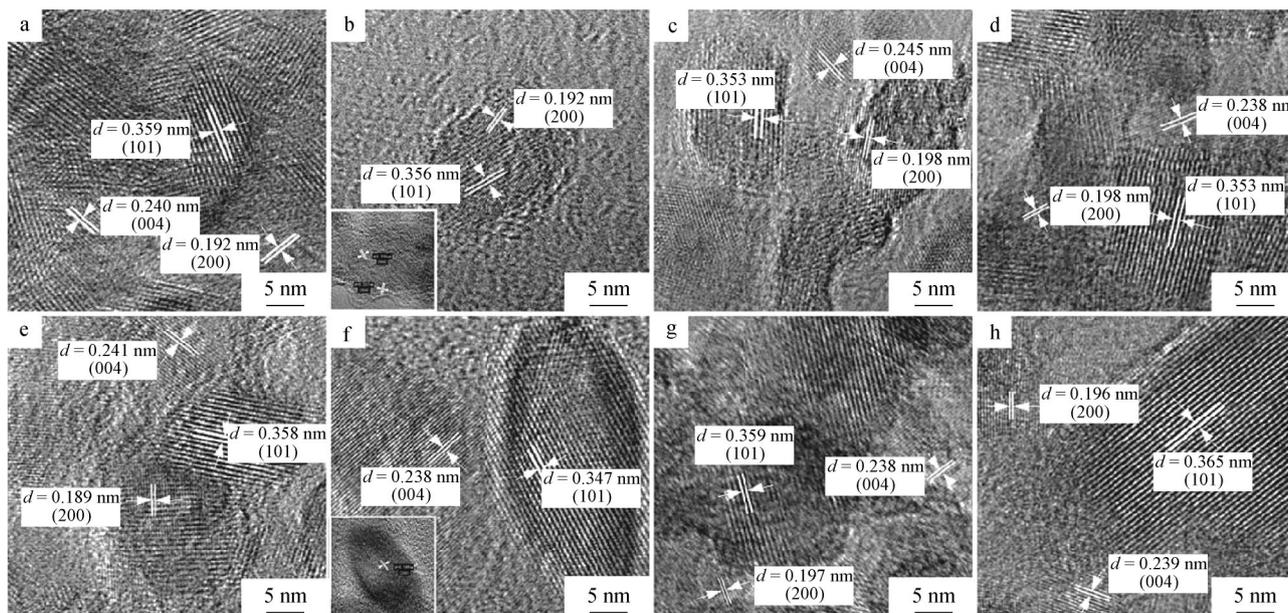


**Fig. 4** TEM image of anatase TiO<sub>2</sub>: **a** Sample 1, **b** Sample 2, **c** Sample 3, **d** Sample 4, **e** Sample 5, **f** Sample 6, **g** Sample 11 and **h** Sample 15

**Fig. 4.** It can be identified that the exposed planes are {100}, {101} and {001} groups. According to XRD results and Debye–Scherer formula, the average grain size or thickness of {100}, {101} and {001} planes can be calculated as shown in Table 2.

Based on the Wulff theory, the {101} plane with low activation energy can account for 94% of the total area [21]. But the surface energy of anatase grain in this paper has decreased due to PEG200 and H<sub>2</sub>O<sub>2</sub> in preparation, and it makes the high surface energy facet {001} and {100} exposed [22]. According to Table 2 and Fig. 4, the evolution of basic shape of anatase TiO<sub>2</sub> particles in Fig. 5 in different pH values can be described as Fig. 6. The model in Fig. 6 can describe morphology change trend of nano-TiO<sub>2</sub> when the pH changes, and its reliability can be proved by the similar morphology characteristic as shown by TEM images in Fig. 2. As shown in Fig. 6, when pH < 11, the

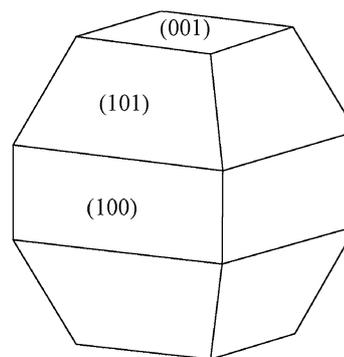


**Fig. 5** Schematic diagram of structural model of anatase grain

sizes of {100}, {101} and {001} planes increase gradually with the increase in pH value, but the size has an obvious change when pH = 11. Compared with Sample 4, Samples 11 and 15 have obvious increase in size due to the lack of modification agent and the higher temperature, respectively.

According to the data in Table 2, the ratio of surface area of {100}, {101} and {001} planes to the total surface area of crystal model in Fig. 6 is calculated as shown in Table 3.

### 3.3.3 Mechanism of grain growth of TiO<sub>2</sub> in hydrothermal preparation

In the hydrothermal condition, Ti<sup>4+</sup> hydrolyzes and forms complex octahedral configuration with H<sub>2</sub>O, OH<sup>-</sup> or O<sup>2-</sup> [23]. The composition of Ti<sup>4+</sup> octahedron varies with the

**Table 2** Average thickness of each plane or grain size (nm)

Samples	{001}	{100}	{101}
1	5.5	6.4	6.3
2	5.6	6.9	6.6
3	5.5	7.4	7.3
4	6.0	7.1	7.8
5	6.9	7.9	8.2
6	25.2	9.3	13.0
11	20.5	10.3	10.7
15	12.5	9.8	10.5

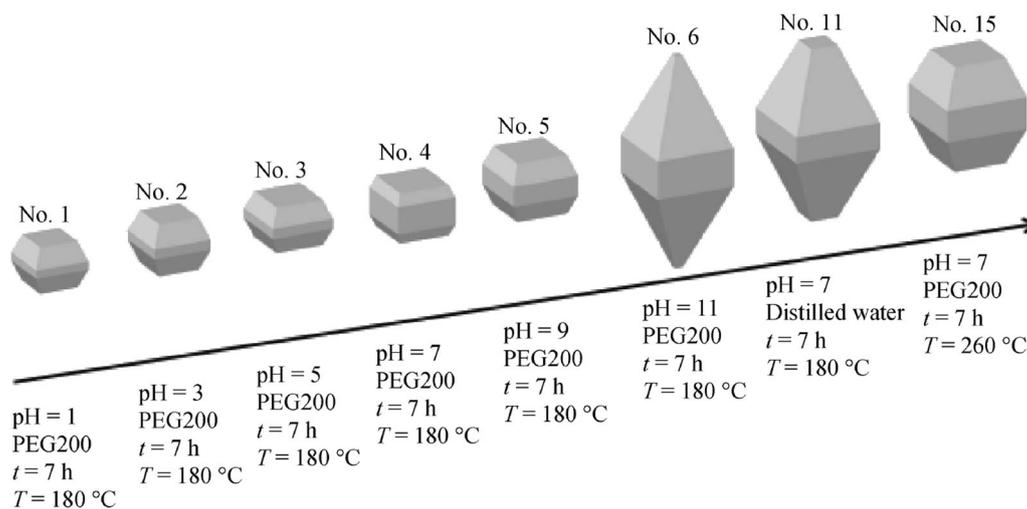


**Fig. 6** Grain model of anatase samples

**Table 3** Surface area ratio of each crystal surface calculated by sample model

Samples	{001}	{100}	{101}
1	0.240	0.144	0.616
2	0.248	0.079	0.647
3	0.289	0.158	0.553
4	0.294	0.384	0.322
5	0.258	0.260	0.482
6	0.003	0.267	0.731
11	0.032	0.193	0.775
15	0.148	0.280	0.572

change in pH value. And there exist three kinds of polymorphism with different connections of octahedral unit. The final structure of anatase is formed by the long chain of bostrychoid polymer connected with edge of octahedrons [24]. With the increase in pH value, the concentration of  $\text{OH}^-$  in the hydrothermal condition increases, which replaces  $\text{O}^{2-}$  on the surface of growth units, leading to the surface hydroxylation [25] and providing the place for hydroxyl reaction. So the average size or thickness of plane in the grain will increase with the increase in pH value when  $\text{pH} < 11$ .

But in the strong alkalic conditions when  $\text{pH} > 11$ , more  $\text{OH}^-$  occupy the position of  $\text{O}^{2-}$  on the surface of growth units and enter into the units to form defects as positive ion vacancies, decreasing the crystal symmetry and increasing the internal energy. So the final product of hydrothermal synthesis in such strong alkalic condition is the brookite with the highest internal energy in the three kinds of polymorphisms of  $\text{TiO}_2$  [26].

### 3.4 Photocatalytic performance of nano-sized $\text{TiO}_2$

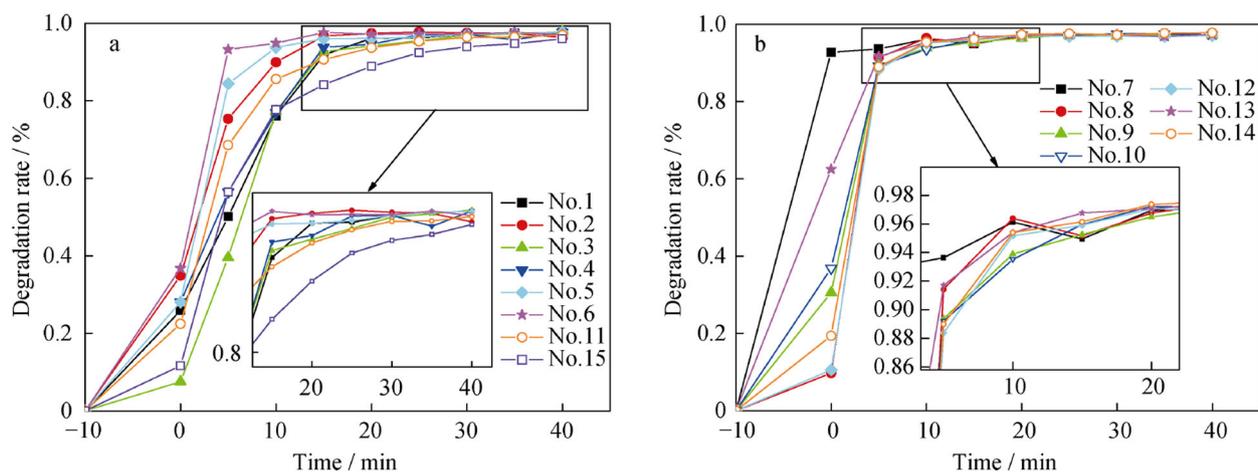
#### 3.4.1 Photocatalytic performance of anatase samples

Figure 7a shows degradation rate of MB over time of Samples 1–6, 11 and 15 under UV radiation. It is obvious that Sample 6 synthesized in weak alkaline environment has strong adsorption ability and the best photocatalytic degradation rate of MB.

When  $\text{TiO}_2$  particles were irradiated by UV light, the electrons on valence band absorbed energy and jumped to conduction band. This jump produces electron–hole pairs which spread to the particle surfaces [27]. A series of redox reactions occur between the electrons or holes and the matter adsorbed on the surface to achieve the purpose of degradation.

The catalytic reduction is prone to take place on {101} facet of anatase for the aggregation of electrons [28, 29]. On the contrary, the catalytic oxidation is favorable on {001} facets for the aggregation of holes. It can be speculated from Table 3 that the high area ratio of {101} facets in Sample 6 may cause more aggregation of electrons on {101} facets. MB molecules receive these electrons on {101} surface to form a reduced state and stay on it. In contrast, Samples 3 and 15 have lower area ratio of {101} facets and weaker adsorption ability, agreeing well with the result in Fig. 7a.

The degradation rate of MB irradiated by UV light for 30 min can reach 90% in Fig. 7a, showing that all anatase samples have good photocatalytic ability. And the degradation rate order of samples irradiated by UV light for 10 min for Samples 1–6 is  $6 > 5 > 2 > 4 > 3 > 1$ , where Sample 6 shows the best photocatalytic property, corresponding to its best adsorption ability. Sample 5 has the best photocatalytic activity in all anatase samples except



**Fig. 7** Degradation rate for methylene blue over time under UV radiation: **a** anatase samples and **b** brookite samples

for Sample 6. There may be two reasons as follows: on the one hand, when pH value of hydrothermal solution is about 9–10, the dispersion of nanoparticles can reach the best state to increase the actual surface area for photocatalytic reaction; on the other hand, Sample 5 has the closest ratio of area of {101} facets to the sum of {001} and {100} facets to achieve the best synergy between them for better degradation effect. Meanwhile, the particle size of Sample 4 is about 10 nm, less than those of Sample 11 and 15, so Sample 4 has larger specific surface area and better photocatalytic activity.

Without irradiation of UV light, the adsorption of MB on the surface of TiO<sub>2</sub> nanoparticles is generally considered to be physical type, which is known as van Edward force adsorption. But with irradiation of UV light, the adsorption of MB on the surface of TiO<sub>2</sub> nanoparticles may change into the chemical type for the trapping of electrons on TiO<sub>2</sub> surfaces by MB molecules in the free state and the subsequent formation of N–H bond as the reduction state, which will be enhanced by the hydrogen bonding of Ti–O bond on the TiO<sub>2</sub> surface. So it is reasonable for Sample 6 to have the strongest adsorption performance due to its highest proportion of {101} surface with the most electronic aggregation for the reduction of MB molecules.

### 3.4.2 Photocatalytic performance of brookite samples

The degradation rate curves of MB under UV light of seven brookite samples are shown in Fig. 7b. Samples 7 and 13 obtained at pH = 13 in hydrothermal solution show strong adsorption ability. Overall, the order of adsorption rate of samples is 7 > 13 > 10 > 9 > 14 > 12 > 8, where the order of adsorption rate of samples with pH value changing but other conditions constant is 7 > 10 > 9 > 8, corresponding to the order of pH value as 13.0 > 12.5 > 12.0 > 11.5. This result indicates that the

adsorption ability of brookite samples will decrease with the decrease in pH value. The degradation rate of brookite samples irradiated by UV light for 10 min can be over 90%. And the photocatalytic effect order of samples at 5 min is 7 > 13 > 8 > 9 > 10 > 14 > 12.

The photocatalytic results show that brookite TiO<sub>2</sub> prepared has a strong degradation capacity of MB, indicating that pure brookite with high crystallinity can be used as a potential effective photocatalyst [30]. This work provides a new insight for TiO<sub>2</sub> photocatalyst design.

## 4 Conclusion

Nano-sized TiO<sub>2</sub> powders with various morphologies and sizes were prepared via hydrothermal synthesis with Ti(SO<sub>4</sub>)<sub>2</sub> as titanium source, PEG200 as modification agent, H<sub>2</sub>O<sub>2</sub> as complexing agent, NaOH and HCl as pH value regulator. Under present preparation conditions, TiO<sub>2</sub> is an anatase phase with pH value less than 11, but is more likely to be a brookite phase with pH value over 11. Nano-sized anatase TiO<sub>2</sub> gradually grows up in some directions with the increase in pH value from 1 to 11. The grain size will increase with the increase in temperature, the removal of modification agent or the prolonging of time, but the phase type will not change only if the pH value of hydrothermal solution is constant.

The photocatalytic performance of nano-sized TiO<sub>2</sub> was measured by the photocatalytic degradation rate of MB under ultraviolet light. Anatase TiO<sub>2</sub> prepared under the weak alkaline hydrothermal environment (pH = 9, 11) has a better photocatalytic degradation performance. It may be the better dispersion with a larger facet area for photocatalytic reaction and the better synergy between {101} facets and {001} or {100} facets. TiO<sub>2</sub> prepared under the strong alkaline hydrothermal environment (pH = 13) has a

brookite phase and shows a strong adsorption ability of MB. By controlling pH value in a hydrothermal solution, nano-sized TiO<sub>2</sub> powders with different phases, sizes and photocatalytic performance can be prepared.

**Acknowledgements** This study was financially supported by the National Natural Science Foundation of China (Nos. 51302322 and 21373273), the Open-End Fund for the Valuable and Precision Instruments of Central South University (No. CSUZC201613), the Open Foundation of Guangdong Provincial Key Laboratory for Technology and Application of Metal Toughening, Guangdong Institute of Materials and Processing (No. GKL201605), the Education Reform Project of Central South University (No. 2016jy03).

## References

- [1] Wold A. Photocatalytic properties of TiO<sub>2</sub>. *Chem Mater.* 1993; 5(3):280.
- [2] Ahmed S, Rasul MG, Martens WN, Brown R, Hashib MA. Heterogeneous photocatalytic degradation of phenols in wastewater: a review on current status and developments. *Desalination.* 2010;261(s1–2):3.
- [3] Yang HG, Sun CH, Qiao SZ, Zou J, Liu G, Smith SC, Cheng HM, Lu GQ. Anatase TiO<sub>2</sub> single crystals with a large percentage of reactive facets. *Nature.* 2008;453(7195):638.
- [4] Liu H, Huang L, Zhang YH, Tu MS. Advances on synthesis of titania nano-materials by liquid chemical methods. *Mater Rev.* 2014;28(15):74.
- [5] Deng XY, Xiang L, Jin Y. Advances on synthesis of nano-powders by liquid chemical methods. *Mod Chem Ind.* 2002;22(1):19.
- [6] Marugán J, Christensen P, Egerton T, Purnama H. Influence of the synthesis pH on the properties and activity of sol–gel TiO<sub>2</sub> photocatalysts. *Int J Photoenergy.* 2008. doi:10.1155/2008/759561.
- [7] Zhou LM, Huang QW, Wang YP. The effect of pH value on preparation of TiO<sub>2</sub> nanoparticles with sol–gel method. *Chin J Process Eng.* 2007;7(3):556.
- [8] Li GQ. Influence of the pH of sol–gel methods on the phase transformation. *Guizhou Sci.* 2005;23(1):30.
- [9] Devi GS, Kumar KAS, Reddy KS. Effect of pH on synthesis of single phase titania (TiO<sub>2</sub>) nanoparticles and its characterization. *Part Sci Technol.* 2014;33(3):219.
- [10] Gao MQ, Chen LJ. Effect of precursor solution pH value on Nb, F-codoped TiO<sub>2</sub>. *J Hebei Norm Univ Sci Technol.* 2014;28(4): 23.
- [11] Ying WLL, Tang Y, Cheng YH, Chen Z. Morphology, crystal structure and adsorption performance of hydrothermally synthesized titania and titanate nanostructures. *Nanoscale.* 2010; 2(12):2751.
- [12] Lai CW, Sreekantan S. Photoelectrochemical properties of TiO<sub>2</sub> nanotube arrays: effect of electrolyte pH and annealing temperature. *J Exp Nanosci.* 2014;9(3):230.
- [13] Ibrahim SA, Sreekantan S. Effect of pH on TiO<sub>2</sub> nanoparticles via sol–gel method. *Adv Mater Res.* 2010;173(1):184.
- [14] Zhou LM, Liu ZR, Huang QW. Preparation and characterization of shape-controlled rutile nano-TiO<sub>2</sub> with low-temperature hydrothermal method. *Semicond Optoelectron.* 2009;30(4):562.
- [15] Wang WB, Yu K. Effect of the reactant concentration and the pH of the system on titanium dioxide particles by hydrothermal synthesis. *J Henan Norm Univ (Natural Science).* 2013;41(1):64.
- [16] Zhu HY, Lan Y, Gao XP, Ringer SP, Zheng ZF, Song DY, Zhao JC. Phase transition between nanostructures of titanate and titanium dioxides via simple wet-chemical reactions. *J Am Chem Soc.* 2005;127(18):6730.
- [17] Yao C, Yang G, Lin XP. Effect of hydrothermal conditions on the microstructure of brookite titanium dioxide. *Chin J Inorg Chem.* 2005;21(12):1821.
- [18] Testino A, Bellobono IR, Buscaglia V, Canevali C, D'Arienzo M, Polizzi S, Scotti R, Morazzoni F. Optimizing the photocatalytic properties of hydrothermal TiO<sub>2</sub> by the control of phase composition and particle morphology. A systematic approach. *J Am Chem Soc.* 2007;129(12):3564.
- [19] Yan N. Effect of surface modification of polymer on the structure and properties of titanium dioxide. Harbin: Heilongjiang University; 2008. 8.
- [20] Gao L, Zheng S, Zhang QH. Nano Titania Photocatalytic Materials and Applications. Beijing: Chemical Industry Press; 2002. 91.
- [21] Zhou L. Study on the influence for 001 facets and 101 facets of anatase TiO<sub>2</sub> in photocatalysis. Shenyang: Institute of Metal Research, Chinese Academy of Sciences; 2013. 16.
- [22] Li JM. Method for preparing anatase TiO<sub>2</sub> nano-particles with {100} planes. China Patent. CN104098132A; 2014.
- [23] Li JX, Wu JQ, Zhuang ZQ. Development of research on TiO<sub>2</sub> nano-particle preparation with hydrothermal method and reaction mechanism. *China Ceram Ind.* 2001;8(2):29.
- [24] Horvat B, Rečnik A, Dražić G. The growth of anatase bipyramidal crystals during hydrothermal synthesis. *J Cryst Growth.* 2012;347(1):19.
- [25] Lin HX, Wang XX, Fu XZ. Properties and distribution of surface hydroxyl groups of TiO<sub>2</sub>. *Prog Chem.* 2007;19(5):665.
- [26] Shi EW. Hydrothermal Crystallography. Beijing: Science Press; 2004. 158.
- [27] Wang X, Li GR, Xu Q. Roles of (001) and (101) facets of anatase TiO<sub>2</sub> in photocatalytic reactions. *Acta Phys-chim Sin.* 2013;29(7):1566.
- [28] Ohno T, Sarukawa K, Matsumura M. Crystal faces of rutile and anatase TiO<sub>2</sub> particles and their roles in photocatalytic reactions. *New J Chem.* 2002;26(9):1167.
- [29] Yu JG, Low JX, Xiao W, Zhou P, Jaroniec M. Enhanced photocatalytic CO<sub>2</sub>-reduction activity of anatase TiO<sub>2</sub> by coexposed 001 and 101 facets. *J Am Chem Soc.* 2014;136(25):8839.
- [30] Zhang J, Yan S, Fu L, Wang F, Yuan MQ, Luo GX, Xu Q, Wang X, Li C. Photocatalytic degradation of rhodamine B on anatase, rutile and brookite TiO<sub>2</sub>. *Chin J Catal.* 2011;32(6):983.